Disturbance observer based MPC for PMSM with multiple disturbances

1st Haifeng Li
School of Automation
Southeast University
Nanjing, China

2nd Shihua Li*
School of Automation
Southeast University
Nanjing, China

3rd Yunda Yan
School of Engineering and Sustainable Development
De Montfort University
Leicester, UK

***Abstract*—This paper proposes an optimisation-based controller for speed regulation of permanent magnet synchronous motor (PMSM) with the safety guarantee on both the current and voltage in the presence of multiple disturbances. A comprehensive disturbance observer (DOB) is designed to estimate the multiple disturbances in PMSM system. By integrating the estimation and future behavior of disturbances into the prediction horizon, an offset-free predictive control law is obtained by solving a constrained optimization problem. Analysis in frequency domain and experimental studies both show that the proposed control approach achieves higher tracking performance with better disturbance rejection.**

***Index Terms*—Permanent magnet synchronous motor (PMSM), speed regulation, model predictive control (MPC), multiple disturbances, disturbance observer (DOB).**

I. Introduction

PERMANENT magnet synchronous motor (PMSM) has been widely applied in highly dynamical and high-precision applications such as traction drives, electric power steering systems, and machine tools due to its high power density, high efficiency and simple structure [1]. However, the existence of uncertainties and disturbances (e.g., unmodeled dynamics, parameter variation, friction force, and load disturbances) results in the difficulty to achieve high control performance in PMSM servo systems and poses the challenge to the traditional control methods, e.g., proportional–integral–derivative (PID) [2].

As one of the advanced control technologies, model predictive control (MPC) is an optimisation-based control strategy which handles variable constraints and ensures the desirable control performance [3]. The main idea of MPC is fully exploiting the model dynamics to predict the future states, and determining the most suitable control action for this moment by solving a finite horizon optimal control problem [4]. However, the industrial applications of the MPC method to some extent were restricted due to the real-time requirement by the online optimization during a long time. In recent years, with the rapid development of hardware and computation, MPC has attracted a great deal of attentions in power electronic system [5], autonomous vehicle system [6]. Besides, MPC methods have been successfully applied to PMSM servo systems due to the safety guarantee on current and voltage and the improvement of the control performance [7].

In spite of the promising features and fruitful results on application of MPC to PMSM servo systems, similar to most of the other advanced feedback control methods, MPC usually asymptotically suppresses the disturbances and uncertainties through a manner of feedback regulation in a relatively slow way [8]. Therefore, disturbance rejection strategies such as DOB or integral control action are introduced into MPC to enhance the disturbance rejection performance of MPC. In [9], by regarding the external disturbance and uncertain parameters in real time as the lumped disturbance, a DOB is designed to obtain the estimation of lumped disturbance and the estimation is embedded into the output prediction to achieve speed regulation and enhance the disturbance rejection in PMSM servo systems. For reducing the speed drop caused by the load torque disturbance, a MPC controller employing integral action is designed to realize zero steady-state error in [10]. Those MPC strategies successfully achieve high performance by regarding disturbances as constant disturbances in the prediction horizon. However, such a treatment is hard to handle disturbances with the dynamic property of higher-order time varying during the wide range operation of the PMSM. Therefore, in order to suppress time-varying disturbances, a reduced-order generalized proportional integral observer (GPIO) is developed to estimate and predict the higher-order time-varying disturbance in PMSM servo systems, and the future behavior of time-varying disturbances is embedded into the output prediction [11].

The above-mentioned MPC control methods only deal with one or two types of disturbances, but multiple disturbances in PMSM servo systems are not considered in most of the existing MPC strategies. In practical PMSM servo systems, multiple disturbances such as current measurement error effect [12], dead-time effect [13] and cogging torque [14] always bring undesirable influences on the closed-loop control performance, and those disturbances are not considered in [10] and [9]. To realize multiple disturbances rejection, a robust controller with comprehensive disturbance observer is proposed in [15], which achieves precise control performance by simultaneously and accurately estimating the multiple disturbances. In [16], a cascaded MPC scheme is developed to solve the problem of reducing the impact of periodic disturbances arising from the

This work is supported by National Natural Science Foundation of China under Grants 62025302 and 61973081. Corresponding author: Shihua Li (lsh@seu.edu.cn)

current sensor offset error on the speed control of PMSM. It is worth noting that the multiple disturbances rejection strategy proposed in [15] motivates this work.

In this paper, by using multiple disturbance estimation technique, an offset-free MPC considering the model of multiple disturbances is proposed to address the speed regulation problem of PMSM servo systems. A comprehensive disturbance observer is designed to estimate multiple disturbances including current measurement error effect, dead-time effect and cogging torque. Quite different from the most of the existing offset-free MPC methods, multiple disturbances are estimated and predicted in the horizon, which significantly improve the prediction accuracy and dynamic performance of PMSM servo systems. Besides, it has been proven that the steady-state error converges to zero in steady state, with the Bode plots to illustrate the valid rejection for disturbances with specific frequencies. Finally, experimental results show the advantages of the proposed control approach.

II. PMSM Model With Multiple Disturbances

According to [15], a discrete-time model of PMSM in the presence of multiple disturbances by using the forward Euler discretization method is given as follows:

$$\begin{cases} \tilde{i}_q(t+1) = h_1\tilde{i}_q(t) + g_1\omega(t) + T_s p\tilde{u}_q(t) + T_s d_q(t) \\ \omega(t+1) = h_2\tilde{i}_q(t) + g_2\omega(t) + T_s d_\omega(t) \end{cases} \tag{1}$$

where $h_1 \triangleq 1-\frac{T_s R_s}{L_q}$, $h_2 \triangleq \frac{3T_s n_p\psi_f}{2J}$, $g_1 \triangleq -\frac{T_s n_p\psi_f}{L_q}$, $g_2 \triangleq 1-\frac{T_s B_v}{J}$, $p \triangleq \frac{1}{L_q}$; T_s is the sampling time and t is the time index; $\tilde{i}_q$ is q-axis current obtained from the measured phase current; $\tilde{u}_q$ is the output voltage of the controller; L_q is q-axis stator inductance, respectively; R_s is the stator resistance; ψ_f is the magnetic flux linkage; J is the rotor inertia; n_p is the number of pole pairs; B_v is the viscous frictional coefficient; ω is the rotor angular velocity; d_q and d_ω are the lumped disturbances of the current loop and the speed loop, respectively, which are given by:

$$\begin{cases} d_q(t) \triangleq a_1\cos(\theta_e+\alpha) + a_2\cos(2\theta_e+\beta) \\ \qquad + b_1\cos(6\theta_e) + \sigma_q \\ d_\omega(t) \triangleq a_3\cos(\theta_e+\alpha) + a_4\cos(2\theta_e+\beta) \\ \qquad + b_2\cos(P\theta_m+\varphi_1) + \sigma_\omega \end{cases} \tag{2}$$

where a_1, a_2, a_3 and a_4 are coefficients related to current measurement error effects; b_1 and b_2 are coefficients related to dead-time effect and cooging torque, respectively; α and β are the constant angular displacements; θ_e is the electrical angle; θ_m is the mechanical angular position of the rotor which is expressed as $\theta_m = \theta_e/n_p$, σ_q and σ_ω are the lumped effects of parametric perturbation and other unmodeled disturbances/uncertainties in the current loop and the speed loop, respectively.

Remark 1. If PMSM is approximately running at a constant speed (ω=ω^*) in the steady state, the electrical angle θ_e will approximately equal $n_p\omega^* T_s t + \alpha_\omega$ where α_ω is a constant angular displacement.

III. Controller Strategy

A. Disturbance Observer Design

In this section, a disturbance observer is utilized to estimate multiple disturbances in current loop and speed loop.

By defining $\varepsilon_{1c} \triangleq \cos(n_p\omega^* T_s)$, $\varepsilon_{1s} \triangleq \sin(n_p\omega^* T_s)$, $\varepsilon_{2c} \triangleq \cos(2n_p\omega^* T_s)$, $\varepsilon_{2s} \triangleq \sin(2n_p\omega^* T_s)$, $\varepsilon_{3c} \triangleq \cos(6n_p\omega^* T_s)$, $\varepsilon_{3s} \triangleq \sin(6n_p\omega^* T_s)$, $\varepsilon_{4c} \triangleq \cos(P\omega^* T_s)$, $\varepsilon_{4s} \triangleq \sin(P\omega^* T_s)$, $u(t) \triangleq \tilde{u}_q(t)$, $x_1(t) \triangleq \tilde{i}_q(t)$, $x_2(t) \triangleq \omega(t)$, $x_3(t) \triangleq a_1\cos(\theta_e+\alpha)$, $x_4(t) \triangleq a_1\sin(\theta_e+\alpha)$, $x_5(t) \triangleq a_2\cos(2\theta_e+\beta)$, $x_6(t) \triangleq a_2\sin(2\theta_e+\beta)$, $x_7(t) \triangleq b_1\cos(6\theta_e)$, $x_8(t) \triangleq b_1\sin(6\theta_e)$, $x_9(t) \triangleq \sigma_q$, $x_{10}(t) \triangleq a_3\cos(\theta_e+\alpha)$, $x_{11}(t) \triangleq a_3\sin(\theta_e+\alpha)$, $x_{12}(t) \triangleq a_4\cos(2\theta_e+\beta)$, $x_{13}(t) \triangleq a_4\sin(2\theta_e+\beta)$, $x_{14}(t) \triangleq b_2\cos(P\theta_m+\varphi_1)$, $x_{15}(t) \triangleq b_2\sin(P\theta_m+\varphi_1)$, $x_{16}(t) \triangleq \sigma_\omega$, an extended system of (1) is represented as follows:

$$\begin{cases} \begin{bmatrix} x_m(t+1) \\ X(t+1) \end{bmatrix} = \begin{bmatrix} A & B_d C_d \\ 0_{14\times 2} & A_d \end{bmatrix} \begin{bmatrix} x_m(t) \\ X(t) \end{bmatrix} + \begin{bmatrix} B \\ 0_{14\times 1} \end{bmatrix} u(t) \\ d(t) = C_d X(t) \\ y(t) = C x_m(t) \end{cases} \tag{3}$$

where $d(t) \triangleq \begin{bmatrix} d_q(t) & d_\omega(t) \end{bmatrix}^T$, $x_m(t) \triangleq \begin{bmatrix} x_1(t) & x_2(t) \end{bmatrix}^T$, $X(t) \triangleq \begin{bmatrix} x_3(t) & x_4(t) & \cdots & x_{16}(t) \end{bmatrix}^T$, $y(t) \triangleq \omega(t)$ and matrices are defined as follows:

$$\begin{aligned} A &= \begin{bmatrix} 1-\frac{T_s R_s}{L_q} & -\frac{T_s n_p\psi_f}{L_q} \\ \frac{3T_s n_p\psi_f}{2J} & 1-\frac{T_s B_v}{J} \end{bmatrix} \\ A_d &= \text{blkdiag}(A_{d1}, A_{d2}, A_{d3}, 1, A_{d1}, A_{d2}, A_{d4}, 1) \\ A_{di} &= \begin{bmatrix} \varepsilon_{ic} & -\varepsilon_{is} \\ \varepsilon_{is} & \varepsilon_{ic} \end{bmatrix}, (i=1,2,3,4),\ B = \begin{bmatrix} \frac{T_s}{L_q} & 0 \end{bmatrix}^T \\ B_d &= \begin{bmatrix} T_s & 0 \\ 0 & T_s \end{bmatrix},\ C_d = \begin{bmatrix} \rho & 0_{1\times 7} \\ 0_{1\times 7} & \rho \end{bmatrix} \\ \rho &= \begin{bmatrix} 1 & 0 & 1 & 0 & 1 & 0 & 1 \end{bmatrix},\ C = \begin{bmatrix} 0 & 1 \end{bmatrix} \end{aligned}$$

Then, the DOB for system (1) is designed as follows:

$$\begin{cases} \begin{bmatrix} \hat{x}_m(t+1) \\ \hat{X}(t+1) \end{bmatrix} = \begin{bmatrix} A & B_d C_d \\ 0_{14\times 2} & A_d \end{bmatrix} \begin{bmatrix} \hat{x}_m(t) \\ \hat{X}(t) \end{bmatrix} + \begin{bmatrix} B \\ 0_{14\times 1} \end{bmatrix} u(t) \\ \qquad + \begin{bmatrix} L_x \\ L_d \end{bmatrix} (x_m(t) - \hat{x}_m(t)) \\ \hat{d}(t) = C_d \hat{X}(t) \end{cases} \tag{4}$$

where L_x and L_d are observer gains.

B. MPC Design with Disturbance Estimation

Embedding disturbance information into the prediction model is critical for the MPC design for PMSM in the presence of multiple disturbances. Besides, inspired by the output regulation theory, a compact approach is adopted here to consider both the disturbance state and reference, which will be specifically deduced in Sec. III-C.

In this subsection, the overall MPC algorithm is first presented as follows:

$$\min_{u_0,\cdots,u_{N-1}} \|x_N - \bar{x}_N\|_F^2 + \sum_{k=0}^{N-1} \|x_k - \bar{x}_k\|_Q^2 + \|u_k - \bar{u}_k\|_R^2 \tag{5a}$$

$$\text{s.t.} \quad \Xi_x x_k + \Xi_u u_k \le \Upsilon \tag{5b}$$

$$x_{k+1} = Ax_k + Bu_k + B_d d_k \tag{5c}$$

$$z_{k+1} = Sz_k \tag{5d}$$

$$d_k = C_d M_d z_k \tag{5e}$$

$$\bar{x}_k = \Pi z_k \tag{5f}$$

$$\bar{u}_k = \Gamma z_k, \ k = 0, 1, \cdots, N \tag{5g}$$

$$x_0 = \hat{x}_m(t) \tag{5h}$$

$$z_0 = \begin{bmatrix} \hat{X}(t)^T & r(t) \end{bmatrix}^T \tag{5i}$$

where $r(t)$ is the reference for speed; x, z and d with subscripts are the variables in horizon; $\bar{x}_k$ and $\bar{u}_k$ are the desired state and input, and the matrix pair (Π, Γ) is the solution of the following algebraic equation:

$$\Pi S = A\Pi + B\Gamma + B_d C_d M_d \tag{6a}$$

$$0 = C\Pi - M_r \tag{6b}$$

and $S \triangleq \text{blkdiag}(A_d, 1)$, $M_d \triangleq \begin{bmatrix} I_{14\times14} & 0_{14\times1} \end{bmatrix}$, $M_r \triangleq \begin{bmatrix} 0_{14\times14} & 1_{14\times1} \end{bmatrix}$, $I_{14\times14}$ is an unit matrix and $1_{14\times1}$ is a column vector whose elements are all 1; Ξ_x, Ξ_u and Υ describe the safety requirement, given by:

$$\Xi_x \triangleq \begin{bmatrix} 1 & 0 & -1 & 0 \\ 0 & 0 & 0 & 0 \end{bmatrix}^T, \ \Xi_u \triangleq \begin{bmatrix} 0 & 1 & 0 & -1 \end{bmatrix}^T$$

$$\Upsilon \triangleq \begin{bmatrix} i_{q\max} & \tilde{u}_{q\max} & -i_{q\max} & -\tilde{u}_{q\max} \end{bmatrix}^T$$

and $Q > 0$ and $R \ge 0$ are the weightings on tracking and control, respectively; F is the terminal weighting, which is the solution of the following Riccati equation

$$F = A^T F A - A^T F B (B^T F B + R)^{-1} B^T F A + Q \tag{7}$$

It is worth noting that the real-time estimates of both PMSM and disturbance states are embedded in the prediction horizon by acting as the initial states, i.e., (5h) and (5i).

The optimal solution to the optimization problem (5) is denoted as:

$$U^*(t) \triangleq \left\{ u_0^*, u_1^*, \cdots, u_{N-1}^* \right\} \tag{8}$$

where the first action u_0^* is utilized to PMSM as the current voltage, that is

$$u(t) = u_0^* \tag{9}$$

At next time, the initial state variable will be updated. Then, the optimization problem (5) is repeated to obtain an optimal voltage.

C. Analysis on Steady-State Error

In what follows, a theoretical analysis on the steady-state error of the PMSM servo system with the appropriate compensation for the multiple disturbance when tracking a constant reference ($r(t) = \omega^*$) is given.

Theorem 1. Suppose that the MPC problem (5) is always feasible and constraint (5b) is always inactive. Then the steady-state error tends to zero, that is, $\lim_{t\to\infty} y(t) = \omega^*$.

Proof. Estimation dynamics is analysed first. By defining $e_{ob}(t) \triangleq \begin{bmatrix} x_m(t)^T & X(t)^T \end{bmatrix}^T - \begin{bmatrix} \hat{x}_m(t)^T & \hat{X}(t)^T \end{bmatrix}^T$, $e_{ob}(t+1)$ can be derived from (3) and (4) as follows:

$$\begin{aligned} e_{ob}(t+1) &= \begin{bmatrix} A & B_d C_d \\ 0_{14\times2} & A_d \end{bmatrix} e_{ob}(t) - \begin{bmatrix} L_x \\ L_d \end{bmatrix} [x_m(t) - \hat{x}_m(t)] \\ &= \Theta_{ob} e_{ob}(t) \end{aligned} \tag{10}$$

where

$$\Theta_{ob} \triangleq \begin{bmatrix} A - L_x & B_d C_d \\ -L_d & A_d \end{bmatrix}$$

It is worth nothing that L_x and L_d can be chosen properly to guarantee the asymptotic convergence of (10) since system (3) is observable.

Tracking dynamics is then able to be deduced. Right multiplying (6a) by z_k, one obtains

$$\bar{x}_{k+1} = A\bar{x}_k + B\bar{u}_k + B_d C_d M_d z_k = A\bar{x}_k + B\bar{u}_k + B_d d_k \tag{11}$$

According to (5c), (5e) and (11), one obtains $\delta x_{k+1} = A\delta x_k + B\delta u_k$ where $\delta x_k \triangleq x_k - \bar{x}_k$, $\delta u_k \triangleq u_k - \bar{u}_k$. Considering the assumption on inactive constraints and letting δu_k as the new decision variable, the MPC problem (5) can be simplified as follows:

$$\begin{aligned} \min_{\delta u_0,\cdots,\delta u_{N-1}} & \|\delta x_N\|_F^2 + \sum_{k=0}^{N-1} \|\delta x_k\|_Q^2 + \|\delta u_k\|_R^2 \\ \text{s.t.} \quad & \delta x_{k+1} = A\delta x_k + B\delta u_k, \ k = 0, 1, \cdots, N \\ & \delta x_0 = \hat{x}_m(t) - \bar{x}_0 \end{aligned} \tag{12}$$

Based on the classical optimal control theory, the controller (12) can be explicitly computed as

$$\delta u_0^* = K_{MPC} \delta x_0 \Leftrightarrow u(t) = K_{MPC}(\hat{x}_m(t) - \bar{x}_0) + \bar{u}_0 \tag{13}$$

where $K_{MPC} \triangleq (R + B^T F B)^{-1} B^T F A$. Taking the controller (13) into the extended system (3) will get

$$\begin{aligned} x_m(t+1) = & Ax_m(t) + BK_{MPC}(\hat{x}_m(t) - \bar{x}_0) \\ & + B\bar{u}_0 + B_d C_d M_d z(t) \end{aligned} \tag{14}$$

where $z(t) \triangleq \begin{bmatrix} X(t)^T & r(t) \end{bmatrix}^T$.

By defining $e_{tr}(t) \triangleq x_m(t) - \Pi z(t)$, $e_{ob1}(t) \triangleq x_m(t) - \hat{x}_m(t)$, $e_{ob2}(t) \triangleq X(t) - \hat{X}(t)$ and keeping (6a) in mind, then $e_{tr}(t+1)$ is computed as:

$$\begin{aligned} e_{tr}(t+1) = & \Theta_{tr} e_{tr}(t) - BK_{MPC} e_{ob1}(t) \\ & + (BK_{MPC}\Pi - B\Gamma)\Lambda e_{ob2} \end{aligned} \tag{15}$$

where $\Theta_{tr} \triangleq A + BK_{MPC}$ and $\Lambda \triangleq \begin{bmatrix} I_{14\times14} & 0_{14\times1} \end{bmatrix}^T$. By (10) and (15), one obtains

$$\begin{bmatrix} e_{tr}(t+1) \\ e_{ob}(t+1) \end{bmatrix} = \begin{bmatrix} \Theta_{tr} & \star \\ 0_{16\times2} & \Theta_{ob} \end{bmatrix} \begin{bmatrix} e_{tr}(t) \\ e_{ob}(t) \end{bmatrix} \tag{16}$$

where $\star$ is a constant matrix. Noting that Θ_{tr} is Hurwitz due to the Riccati equation (7), the closed-loop system (16) is asymptotically stable, which implies that $\lim_{t\to\infty} e_{tr}(t) = 0 \Rightarrow \lim_{t\to\infty} y(t) = \omega^*$. This completes the proof.

IV. Frequency-Domain Analysis for Disturbance Estimation and Rejection

Frequency-domain analysis for the proposed controller is significant to show the effectiveness of the estimation and rejection for disturbances mentioned in Section II. In what follows, frequency-domain analysis of the disturbances in the current and speed channels are proposed.

To show the disturbance estimation performance, the estimation transfer function from d_q to $e_q = d_q - \hat{d}_q$ and from d_ω to $e_\omega = d_\omega - \hat{d}_\omega$ are defined as:

$$G_q(z) \triangleq \frac{d_q(z) - \hat{d}_q(z)}{d_q(z)},\ G_\omega(z) \triangleq \frac{d_\omega(z) - \hat{d}_\omega(z)}{d_\omega(z)} \tag{17}$$

Then the Bode plots of current-loop disturbance estimation error $G_q(z)$ and speed-loop disturbance estimation error $G_\omega(z)$ with different ω^* are shown in Fig. 1 and Fig. 2, respectively. Table I shows the specific frequencies of multiple disturbances at different desired speeds. As shown in Fig. 1, the disturbance estimation errors of current measurement error and dead time effect decrease obviously at specific frequencies, which indicates that the DOB estimates the multiple disturbances precisely. Besides, it can be shown in Fig. 2, that the disturbance caused by cogging torque and current measurement error can be estimated with accuracy.

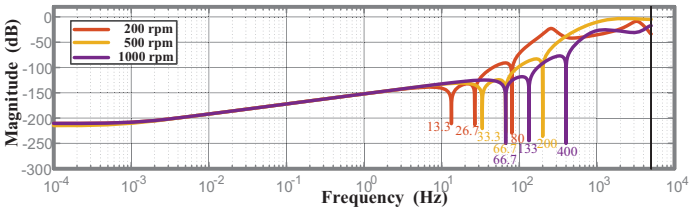

Fig. 1. Bode plots of disturbance estimation error in current loop with different ω^*.

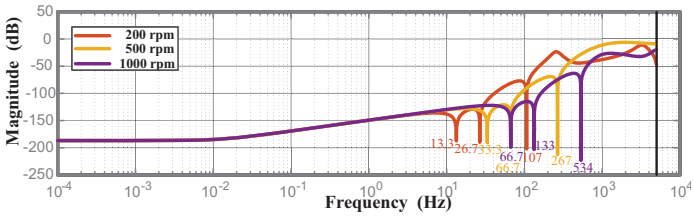

Fig. 2. Bode plots of disturbance estimation error in speed loop with different ω^*.

TABLE I
Specific frequencies of multiple disturbances under different speeds

Desired speed	Offset error	Scaling error	Dead time effect	Cogging torque
200rpm	13.3Hz	26.7Hz	80Hz	107Hz
500rpm	33.3Hz	66.7Hz	200Hz	267Hz
1000rpm	66.7Hz	133Hz	400Hz	534Hz

To study the performance of disturbance rejection, the transfer functions from d_q and d_ω, respectively, to the tracking error $\omega^* - \omega$ are defined as:

$$G_{eq}(z) \triangleq \frac{\omega^*(z) - \omega(z)}{d_q(z)},\ G_{e\omega}(z) \triangleq \frac{\omega^*(z) - \omega(z)}{d_\omega(z)} \tag{18}$$

where the desired speed is set as 500rpm. Then the Bode plots of transfer functions in (18) with different $Q:R$ and different observer poles are shown in Fig. 3-6. As shown in Fig. 3 and Fig. 4, the tracking error deceases at specific frequencies (33.3Hz, 66.6Hz, 200Hz and 267Hz) with the increase of $Q:R$ when the observer poles are all placed at -50. It can be shown in Fig. 5 and Fig. 6 that the tracking error is getting smaller with larger observer poles when $Q:R$ is set as $100I$.

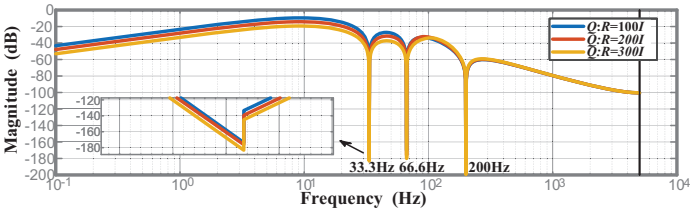

Fig. 3. Bode plots of tracking error in current loop with different $Q:R$.

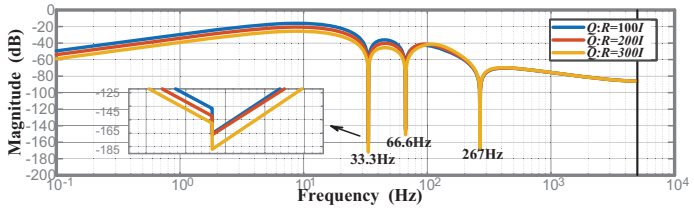

Fig. 4. Bode plots of tracking error in speed loop with different $Q:R$.

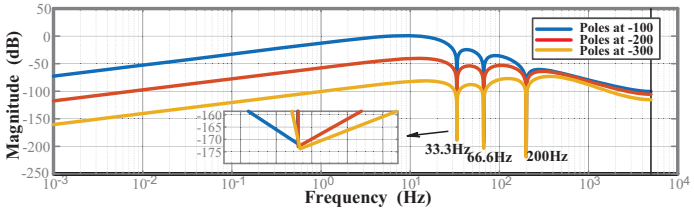

Fig. 5. Bode plots of tracking error in current loop with different poles of observer.

V. Experiment Studies

In this section, the disturbance observer based MPC method is to be validated by experimental studies. The experimental

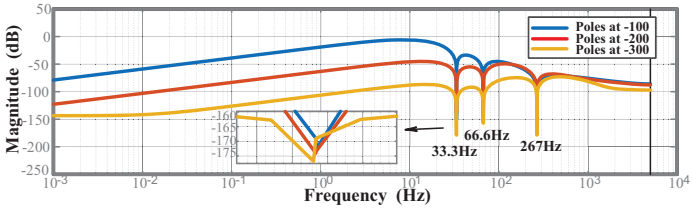

Fig. 6. Bode plots of tracking error in speed loop with different poles of observer.

setup is shown in Fig. 7(a), and its configuration is given in Fig. 7(b). The experimental setup consists of a host PC, a load adjusting device, a PMSM and an integrated controller board. The integrated controller board includes dual processor and a DSP (TMS320F28335) motion control board.

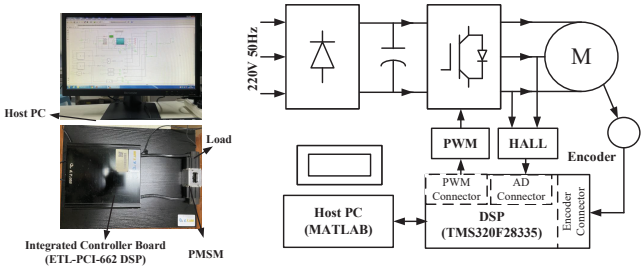

(a) (b)

Fig. 7. Experimental system: (a) setup. (b) configuration.

The parameters of the PMSM are as follows: number of pole pairs $n_p = 4$, number of slots $P = 32$, rotor flux linkage $\psi_f = 0.0192\text{Wb}$, stator inductances $L_d, L_q = 0.4\text{mH}$, stator resistance $R_s = 0.72\Omega$, rotor inertia $J = 7.06 \times 10^{-4}\text{kg} \cdot \text{m}^2$, and viscous friction coefficient $B_v = 3.5 \times 10^{-4}\text{N} \cdot \text{m} \cdot \text{s/rad}$. The current constraint is 10A. The setting value of speed is given as 500rpm, and the sampling period T_s is 0.1ms. The controller parameters of MPC are given as $N = 5$, $R = 0.01$, $Q = 500I$ where I is identity matrix. The parameters of DOB are designed by using the "place" instruction in MATLAB. Eigenvalues of (4) are placed at -500 for tuning simplicity.

A. Nominal Control Performance

In this case, the nominal control performance of three controllers are tested with multiple disturbances.

It is worth noting that the current measurement error effects are much larger than dead-time effect and cogging torque in this experimental device, therefore the proposed control strategy mainly rejects the current measurement error effects.

As shown in Fig. 8, the MPC+ESO and PID have much more fluctuations in the steady state under multiple disturbances. It is observed in Fig. 9 that the proposed MPC+DOB is well tuned to behave satisfactory nominal control performance while satisfying the current constraint in the whole regulation process. The amplitude spectra of tracking error is shown in Fig. 10. It can be seen that the multiple disturbances (33.333Hz and 66.666Hz while motor speed is 500rpm) of the system with MPC+DOB are suppressed to a large extent.

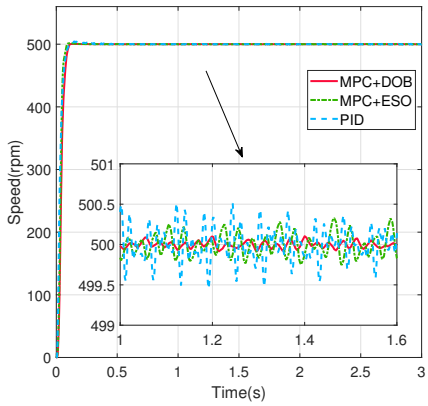

Fig. 8. Speed response at a desired speeds of 500rpm.

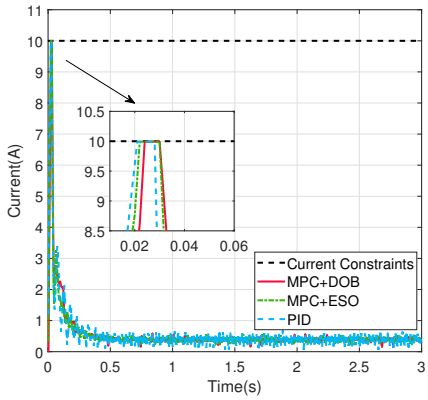

Fig. 9. Current response at a desired speeds of 500rpm.

Detailed quantitative data for performance comparisons of three cases are given in Table II. It can be observed from Table II that fluctuations on the speed curves of PID are relatively larger than those of MPC+ESO and MPC+DOB. The effects of disturbances can be completely attenuated if and only if the internal models of disturbances are incorporated into the controller design. This indicates that the PID controller can only remove the offset caused by constant/step disturbances since the integral action serves as the internal model of this kind disturbances.

TABLE II
DYNAMIC-STATE AND STEADY-STATE PERFORMANCES

Index	PID	MPC+ESO	MPC+DOB
Overshoot (%)	0.86	0.29	0.09
Settling time (s)	0.11	0.10	0.09
Offset error (r/min)	0.01	0.00	0.00
Fluctuation (r/min)	0.59	0.29	0.12
Fluctuation (%)	0.12	0.06	0.02

B. Robustness Against Step Load Torque

The robustness against step load torque $T_L = 0.4\text{N} \cdot \text{m}$ while the desired speed is given by 500rpm is respectively

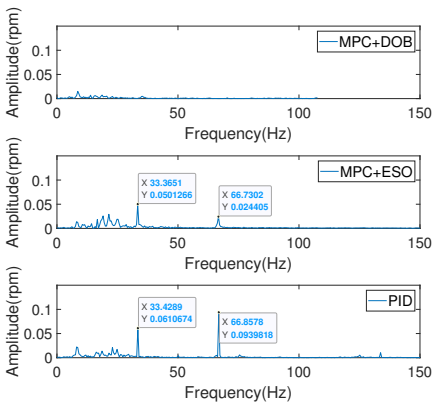

Fig. 10. Amplitude spectra of steady-state tracking error at a desired speeds of 500rpm.

tested in this case. The step load torque is applied at 3s. MPC+DOB, MPC+ESO and PID are compared in this case.

Fig. 11 are speed responses under load torque. As shown in Fig. 11, MPC+DOB has the smallest maximum angular velocity drop compared with MPC+ESO and PID.

More detailed quantitative performance index comparisons of PID, MPC+ESO and MPC+DOB are provided in Table III. It can be observed from Table III that the speed drop of PID are relatively larger than those of MPC+ESO and MPC+DOB.

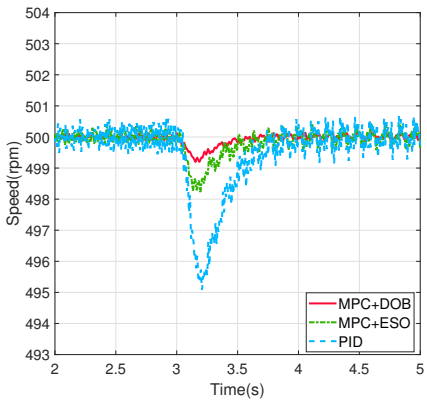

Fig. 11. Speed response with load torque at a desired speeds of 500rpm.

TABLE III
DISTURBANCE REJECTION PERFORMANCES AGAINST LOAD TORQUES

Index	PID	MPC+ESO	MPC+DOB
Decrease (r/min)	4.91	0.42	0.13
Recovery time (s)	0.50	0.43	0.38
Offset Error (r/min)	0.02	0.01	0.00
Fluctuation (r/min)	0.77	0.43	0.16
Fluctuation (%)	0.15	0.09	0.03

VI. CONCLUSION

In this paper, a DOB based MPC method has been proposed to achieve high control performance of PMSM servo systems in the presence of multiple disturbances as well as overcurrent protection. A DOB has been designed to estimate multiple disturbances, which is fully exploited during the prediction horizon to substantially improve the prediction accuracy. Then, a MPC with the disturbance estimate based prediction correction has been designed. The proposed control method has taken current and voltage constraints into account, and at the same time, reacts swiftly to reject multiple disturbances. The implementation and experimental results have shown that the method proposed in this paper shows a faster transient response and a better disturbance rejection ability.

REFERENCES

[1] R. Krishnan, "Electric motor drives: Modeling, analysis, and control," *Prentice Hall*, Jan. 2001.

[2] A. V. Sant and K. R. Rajagopal, "PM synchronous motor speed control using hybrid fuzzy-PI with novel switching functions," *IEEE Transactions on Magnetics*, vol. 45, no. 10, pp. 4672–4675, Oct. 2009.

[3] U. Maeder, F. Borrelli, and M. Morari, "Linear offset-free model predictive control," *Automatica*, vol. 45, no. 10, pp. 2214–2222, Oct. 2009.

[4] S. Vazquez, J. Rodriguez, M. Rivera, L. G. Franquelo, and M. Norambuena, "Model predictive control for power converters and drives: Advances and trends," *IEEE Transactions on Industrial Electronics*, vol. 64, no. 2, pp. 935–947, Nov. 2017.

[5] S. Vazquez, J. I. Leon, L. G. Franquelo, J. Rodriguez, H. A. Young, A. Marquez, and P. Zanchetta, "Model predictive control: A review of its applications in power electronics," *IEEE Industrial Electronics Magazine*, vol. 8, no. 1, pp. 16–31, Mar. 2014.

[6] P. Falcone, F. Borrelli, J. Asgari, H. Tseng, and D. Hrovat, "Predictive active steering control for autonomous vehicle systems," *IEEE Transactions on Control Systems Technology*, vol. 15, no. 3, pp. 566–580, Jan. 2007.

[7] H. Liu and S. Li, "Speed control for PMSM servo system using predictive functional control and extended state observer," *IEEE Transactions on Industrial Electronics*, vol. 59, no. 2, pp. 1171–1183, Feb. 2012.

[8] J. Yang, W. Zheng, S. Li, B. Wu, and M. Cheng, "Design of a prediction-accuracy-enhanced continuous-time MPC for disturbed systems via a disturbance observer," *IEEE Transactions on Industrial Electronics*, vol. 62, no. 9, pp. 5807–5816, Sep. 2015.

[9] M. Zhou, X. Liu, and S. Li, "Composite single-loop model predictive control design for PMSM servo system speed regulation based on disturbance observer," *Proceedings of the 32nd 2020 Chinese Control and Decision Conference (Ccdc 2020)*, pp. 2886–2892, Aug. 2020.

[10] S. Chai, F. Wang, and E. Rogers, "Model predictive control of a permanent magnet synchronous motor with experimental validation," *Control Engineering Practice*, vol. 21, no. 11, pp. 1584–1593, Nov. 2013.

[11] J. Liu, J. Yang, and S. Li, "Single-loop robust predictive speed control of PMSM system with overcurrent protection: A disturbance preview approach," *2021 IEEE International Conference on Predictive Control of Electrical Drives and Power Electronics (PRECEDE)*, pp. 645–650, Nov. 2021.

[12] D. W. Chung and S. K. Sul, "Analysis and compensation of current measurement error in vector-controlled AC motor drives," *IEEE Transactions on Industry Applications*, vol. 34, no. 2, pp. 340–345, Mar. 1998.

[13] S. H. Hwang and J. M. Kim, "Dead time compensation method for voltage-fed PWM inverter," *IEEE Transactions on Energy Conversion*, vol. 25, no. 1, pp. 1–10, Mar. 2010.

[14] N. Bianchi and S. Bolognani, "Design techniques for reducing the cogging torque in surface-mounted PM motors," *IEEE Transactions on Industry Applications*, vol. 38, no. 5, pp. 1259–1265, Sep. 2002.

[15] Y. Yan, J. Yang, Z. Sun, C. Zhang, S. Li, and H. Yu, "Robust speed regulation for PMSM servo system with multiple sources of disturbances via an augmented disturbance observer," *IEEE/ASME Transactions on Mechatronics*, vol. 23, no. 2, pp. 769–780, Apr. 2018.

[16] S. Chai, F. Wang, and E. Rogers, "A cascade MPC control structure for a PMSM with speed ripple minimization," *IEEE Transactions on Industrial Electronics*, vol. 60, no. 8, pp. 2978–2987, Aug. 2013.